

Relationship between monthly rainfall in northwest Iberian Peninsula and North Atlantic sea surface temperature

M. N. Lorenzo,^{a*} I. Iglesias,^a J. J. Taboada^b and M. Gómez-Gesteira^a

^a Campus de Ourense, University of Vigo, E-32004 Ourense, Spain

^b Meteogalicia, Santiago de Compostela, Spain

ABSTRACT: This study assesses the relationship between monthly North Atlantic sea surface temperature anomalies (SSTAs) and a regional index of rainfall (NWIPR) in northwest Iberian Peninsula during the period 1951–2006 by means of the Pearson product-moment correlation. Results show a strong influence of SSTA on NWIPR in several months (February, April, May, October and December). The observed persistence of this influence up to 2-months in advance can be used for monthly predictions of rainfall. The most significant areas of the North Atlantic were clustered to be used as input variables in linear regression models. Correlations up to 0.59 between observed and predicted rainfall anomalies were obtained. Predictability ranged from 76 to 86% when considering rainfall as a discrete predictand. Copyright © 2009 Royal Meteorological Society

KEY WORDS northwest Iberian Peninsula; rainfall; sea surface temperatures; North Atlantic; linear regression; predictability

Received 8 July 2008; Revised 17 April 2009; Accepted 22 April 2009

1. Introduction

Sea surface temperature (SST) plays a key role in the control of climate due to the processes of evaporation, precipitation and atmospheric heating. Anomalies in the atmospheric variables are often associated to sea surface temperature anomalies (SSTA), at least at a monthly or seasonal time scale. Due to the high inertia of the sea, SSTA is a reliable variable to be used as a climatic predictor. Actually, different studies carried out during the last decades have reported that SSTs can be of some utility in monthly or seasonal rainfall prediction, owing to the ocean's large thermal mass (Barnston, 1994). The importance of this variable is highlighted in the seasonal forecast field and, of course, in the climate models, in which the influence of the ocean is indispensable.

Previous works have shown the influence of anomalies in sea level pressure and precipitation variability on changes in the SST (Rowell, 1998) in the Pacific area. Other works have analysed the influence of the global-scale SST patterns on continental precipitation and temperature (Barnston and Smith, 1996; Rodwell *et al.*, 1999; Drévilion *et al.*, 2001; Rodwell and Folland, 2002). In particular, North Atlantic SSTs have been related to precipitation in different European areas, namely, in Sardinia, Italy (Delitala *et al.*, 2000); in southwest England (Phillips and McGregor, 2002); in Iceland (Phillips and Thorpe, 2006); in Iberian Peninsula and Northern Africa (Rodríguez-Fonseca *et al.*, 2006).

It is a well-known fact that European climate variability is hard to forecast because the area is located in the mid-latitude belt. In these latitudes, the absence of a forcing similar to El Niño Southern Oscillation, where the coupling atmosphere–ocean is very strong, makes the identification of a clear connection between atmosphere and ocean a complex task. In particular, Galicia (Figure 1) is located in the western coast of Europe ranging in latitude from 42°N to about 44°N. Previous studies (Cabanas and Alvarez, 2005; Lorenzo and Taboada, 2005; deCastro *et al.*, 2006, 2008a, 2008b) have proved that some climatic variables such as coastal upwelling (directly linked to wind speed) and rainfall do not depend on a single index.

Galicia has a maritime climate, but the most part of the rain is concentrated between October and March when receive the visit of cold fronts travelling across the North Atlantic. This period of rainfall prevents water shortages during summertime. Nevertheless, soil characteristics make the region very dependent on the annual rainfall cycle (Martínez Cortizas and Pérez Alberti, 2000). This sensitivity makes the characterisation of the variables that influence rainfall an interesting task from the scientific and social viewpoints. Moreover, Galician rivers in general and the Miño River in particular are especially important in terms of discharge compared with the basin extent. The ratio between run-off and catchment area (in $\text{Hm}^3 \text{yr}^{-1} \text{km}^{-2}$) is 0.75 for the Miño River (www.ospar.org) in this way, while Galicia represents only about 6% of the area of Spain, it provides about 20% of the hydroelectric energy, although with a considerable interannual

* Correspondence to: M. N. Lorenzo, Campus de Ourense, University of Vigo, E-32004 Ourense, Spain.
E-mail: nlorenzo@uvigo.es

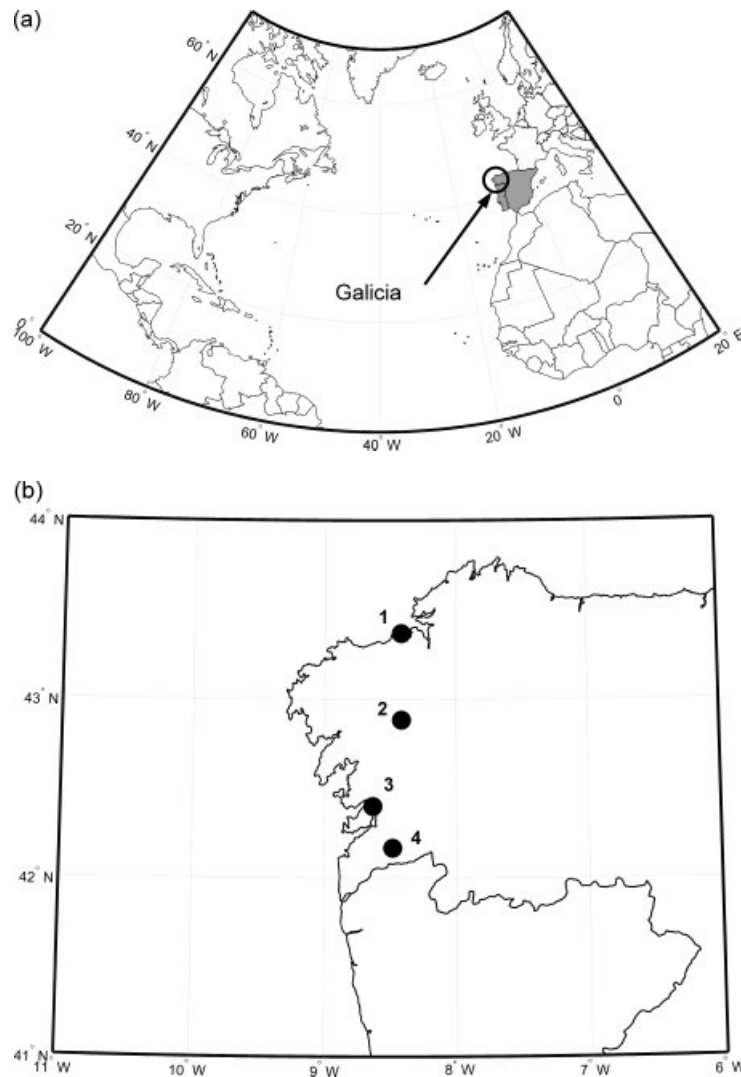


Figure 1. (a) Location of Galicia and spatial extent of sea surface temperature data considered in this study. (b) Location of meteorological stations used in the study; 1, the A Coruña station; 2, the Santiago station; 3, the Salcedo station; 4, the Pontearreas station.

variability (6332 ± 720 GWh during 1999–2004 according to Red Eléctrica de España (www.ree.es). According to the OSPAR commission (www.ospar.org), the Miño River is characterised by an interannual variability in run-off that is close to 40%. This level of variability, which can produce dramatic effects in terms of energy production, can likely be partially mitigated improving the ability to forecast Galician rainfall (deCastro *et al.*, 2006). Thus, a potential degree of monthly or seasonal forecast in the area of northwest (NW) Spain based on SSTA will improve hydroelectric productivity and avoid summer water shortages.

The main objective of this study is to describe the relationship between monthly values of rainfall anomaly for Galicia and concurrent variations in North Atlantic SST. Second, the possibility of elaborate monthly forecast using North Atlantic SST values will be explored.

The article is organised as follows. Details regarding the study area are provided in Section 2. Data and methodology used in this study are described in Section 3 that includes a detailed account of the used field

significance testing procedure. Results are presented and discussed in Section 4 and 5, respectively. Finally, conclusions are drawn in Section 6.

2. Study area

Galicia (42°N to 44°N , 10.5°W to 6°W) is located in the humid zone of the Iberian Peninsula (Figure 1). The area is surrounded by sea for approximately 50% of its perimeter and it constitutes the westernmost part of Europe, being exposed to the periodic passage of Atlantic storms.

Annual rainfall totals at locations close to coast on the southwest region fall within the narrow range of 1600–1900 mm, in the interior, the annual precipitation totals oscillate between 800 and 1000 mm. The precipitation in Galicia is characterized by a maximum in winter, from November to February and a minimum in summer, from June to August (Lorenzo and Taboada, 2005; deCastro *et al.*, 2006). This rain pattern is negatively correlated with the temperature pattern as corresponding to this latitude (Alvarez *et al.*, 2005). The area is characterised

by a wind regime depending on the seasonal migration of the Azores high. Thus, southwesterly winds are prevalent during the wet season and northerly winds during the dry season (Gomez-Gesteira *et al.*, 2006; Alvarez *et al.*, 2008). For a complete study on the weather types in the area, see Lorenzo *et al.* (2008).

3. Data and methods

SST data were provided by the NOAA/OAR/ESRL PSD, Boulder, Colorado, USA, from their Web site at <http://www.cdc.noaa.gov/>. The extended reconstructed SST (ERSST; NOAA_ERSST_V2) was constructed using the most recently available International Comprehensive Ocean–Atmosphere Data Set SST data and improved statistical methods that allow stable reconstruction using sparse data. This monthly analysis begins January 1854, but because of sparse data, the analysed signal is heavily damped before 1880. Afterward, the strength of the signal is more consistent over time. Monthly averaged data are located in a $2^\circ \times 2^\circ$ grid. In the present study, data were taken from 1 January 1951 through December 2006. Taking into account the geographical position of Galicia, monthly SST will be only considered for the region $0\text{--}70^\circ\text{N}$ and $100^\circ\text{W}\text{--}20^\circ\text{E}$ [Figure 1(a)]. This restriction does not necessarily imply that the existence of significant relationships is confined to this area.

Monthly precipitation data in mm from 1951 to 2006 were obtained from the database CLIMA of the University of Santiago de Compostela with data from the *Agencia estatal de Meteorología* and the Regional Government of Galicia that are distributed throughout the territory. These data underwent a quality control procedure with substitutions made for poor quality and some missing data, similar to the one used in the National Climate Data Center, National Oceanic and Atmospheric Administration (NOAA) for Global Historical Climate Network database (Peterson *et al.*, 1998). Quality control for these series of data gave a result of only 0.01% of missing data and 90% of correlation with neighbour stations.

Table I summarises the geographic characteristics of the meteorological stations chosen in this study. Averaging rainfalls corresponding to the four stations can constitute a valid procedure in our study because the four time series are closely correlated, being the lowest correlation ($r^2 = 0.90$) observed between stations 1 and 4.

Table I. Meteorological stations with rainfall data from 1951 to 2006.

Station	Altitude (m)	Latitude	Longitude
1 A Coruña	58	43°22'	−8°25'
2 Santiago	367	42°53'	−8°25'
3 Salcedo	40	42°24'	−8°38'
4 Pontearreas	50	42°10'	−8°29'

Monthly rainfall totals were expressed as anomalies relative to the period 1951–2006. The rainfall anomaly index North West Iberian Peninsula Rainfall (NWIPR) (Phillips and McGregor, 2001, 2002) was adopted in the present study. This *nondimensional* index, which is defined as follows,

$$\text{NWIPR} = 100 \sum_1^N (X/\bar{X})$$

provides an adequate first approximation of monthly variations in the studied area. X is the monthly rainfall anomaly at one station in mm, \bar{X} is the station's mean annual rainfall in mm and N is the number of stations.

The Pearson product-moment correlation coefficient r was considered to quantify the linear association between the SSTA of each $2^\circ \times 2^\circ$ grid square and NWIPR. The coefficient's significance was assessed to be greater than 95% by means of Student's t test.

As it is possible to obtain a statistically significant correlation by simply correlating two random number series, we applied a test for field significance considering the properties of finiteness and interdependence of the spatial grid. Finiteness is defined as the dimensionality of the grid. Following Phillips and McGregor (2002), finiteness was calculated assuming that there are two possible outcomes when calculating a correlation coefficient for any given grid square: The coefficient is significant at the 95% confidence level (outcome a); the coefficient is not significant at the 95% confidence level (outcome b). This high significance was chosen to avoid confusion with random correlations in the posterior calculations. This procedure is repeated n times, where n is the number of grid squares in the data matrix. A two-outcome process ($a + b$) that is repeated n times has a binomial probability distribution. The binomial expansion of $(a + b)^n$ can thus be used to determine the number of grid squares that must have statistically significant correlations at the 95% confidence level from a total of n such that the probability of the result occurring by chance is less than 0.05 (Livezey and Chen, 1983). The number of independent tests conducted by month in this study is about 1471, thus the minimum percentage of grid squares that must have statistically significant correlations at the 95% level is on the order of 5% following the diagram given by Livezey and Chen's (1983). On the other hand, the value of SST of one grid square is not independent of the value of the SST of neighbouring grid squares. In this way, the limit of 5% is too low. Therefore, a stronger test must be applied.

Monte Carlo simulations (Livezey and Chen, 1983; Wilks, 1995) have been commonly used to test for field significance in a spatially correlated matrix. The Monte Carlo simulations were conducted using SST data in August and December that correspond to the month with the lowest and highest rainfall, respectively (Figure 2). SST data were available for 1471 grid squares in the study area.

For the Monte Carlo simulation, the precipitation series were replaced with a Gaussian noise series generated

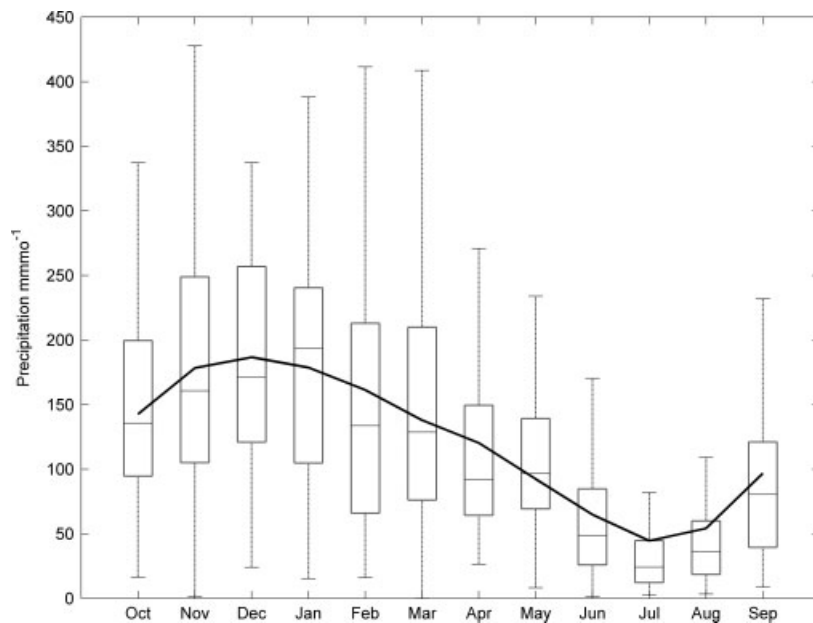


Figure 2. Annual hydrologic cycle variability for the monthly precipitation in Galicia from 1951 to 2006. Solid line represents the monthly average, solid line inside each box represents the median value for each month, the lower/upper whisker represents the minimum/maximum rainfall and the lower/upper box limits represent the first/third quartile, respectively.

from a normal population whose mean and variance are identical to that of the series during the period 1951–2006. The August and December values of this Gaussian noise series were then correlated with the corresponding SSTA values of the 1471 grid squares and the number of coefficients statistically significant at the 0.05 level noted. This procedure was iterated 1471 times, using a new Gaussian noise series for each simulation. A histogram was constructed showing the number of statistically significant grid squares across the 1471 trials from which the critical percentage required for field significance at the 95% confidence level was estimated around of 20% in both cases.

As the interdependence criterion is much more restrictive than the finiteness one, only the first criterion will be considered from now on. Clusters corresponding to the isolated regions with the highest correlation will be calculated as follows: (1) the ocean areas with SSTA: NWIPR correlation higher than 95% for each month at different lags from 0 to 3 months will be marked; (2) the common areas corresponding to the four lags will be identified as the monthly clusters. Two central clusters will be calculated for every significant month fulfilling the interdependence criterion. The cluster means will be used as the input variables of linear regression models that specify rainfall anomaly from SSTA.

4. Results

4.1. Rainfall characteristic of study area

Figure 2 shows the annual hydrologic cycle corresponding to averaging rainfalls of the period 1951–2006; we applied a moving window mean of two months to smooth the graphic. Two clearly defined seasons (wet and dry)

can be distinguished as mentioned above. Nevertheless, the rainfall regime shows important interannual variations (Table II), which can be characterised in terms of the mean, standard deviation and the coefficient of variation (CV) ($CV_i = 100 \times \sigma(R_i) / \langle R_i \rangle$), where R is the rainfall, the subscript i refers to the month and $\langle R \rangle$ and $\sigma(R)$ are the mean value and the standard deviation, respectively. The CV is a dimensionless number. CV ranges from 56% in January to 87% in July, tending to be higher during the dry season.

4.2. Relationship between SSTA and rainfall

The concurrent and lagged correlation between SSTA and NWIPR are shown in Table III, where the month and

Table II. Monthly mean (mm), standard deviation (mm) and the coefficient of variation (CV is a dimensionless number) for the period 1951–2006 of the averaging rainfalls corresponding to the four stations described in Table I.

Month	Mean	Standard deviation	CV
January	195	109	56
February	164	113	69
March	150	107	71
April	117	77	66
May	107	62	58
June	59	44	75
July	30	26	87
August	45	33	73
September	94	63	67
October	172	115	67
November	192	112	58
December	205	135	66

Table III. SSTA: NWIPR field significance testing.

Month	Percentage significant (LAG 0)	Percentage significant (LAG 1)	Percentage significant (LAG 2)	Percentage significant (LAG 3)
January	13.5	32.0*	6.0	16.2
February	32.2*	11.2	15.7	14.3
March	16.6	23.5*	31.2*	7.8
April	22.2*	20.5*	11.8	0.6
May	27.8*	7.0	6.9	15.2
June	11.1	12.2	9.2	6.8
July	13.8	11.8	7.9	35.0*
August	5.9	1.3	57.8*	14.1
September	3.0	67.8*	12.2	1.8
October	68.7*	6.4	3.0	5.0
November	7.5	5.5	6.7	25.7*
December	20.6*	5.8	39.7*	14.8

SSTA, sea surface temperature anomalies; NWIPR, regional index of rainfall.

Months and delays verifying the test for field significance at 0.1 level are marked with an asterisk.

lags that verify the test for field significance at 0.1 level are marked with an asterisk. Only five months (February, April, May, October and December) present statistically significant correlation when considering concurrent SSTA: NWIPR values. Nevertheless, December will be excluded from the further study since its significance hardly surpasses the limit fixed by the interdependence criterion and, in addition, no significant correlation was

observed when lagging the analysis. Similar results were previously observed by Phillips and McGregor (2002) in southwest England and Phillips and Thorpe (2006) in Iceland.

The geographic distribution of significant SSTA: NWIPR (Figure 3) is observed to depend on the month under study. Concurrent correlations (first column in Figure 3) will be analysed first. NWIPR in February seems to be negatively correlated with two bands stretching from American coast to the Euro-African region. The first band is located at tropical latitudes and stretches from South America to the Gulf of Guinea. The second one crosses the Atlantic from the Gulf of Mexico to Scandinavia. May is also characterised by a negatively correlated band similar to the upper one observed in February. April is characterised by a tropical band of positive significant correlation between SSTA and NWIPR. This band stretches from the Gulf of Guinea to the American coast reaching the Pacific Ocean. October presents a strong and wide SSTA: NWIPR concurrent correlation with most of the North Atlantic area.

4.3. Use of SSTA to forecast monthly rainfall

The main objective of our work is to establish the basis for a monthly forecast of rainfall in NW Iberian Peninsula. Thus, lagged SSTA: NWIPR correlations up to three months will be considered in the present study since this is the decay scale that would be expected due to local damping associated to sea–air interaction (Frankignoul *et al.*, 1998).

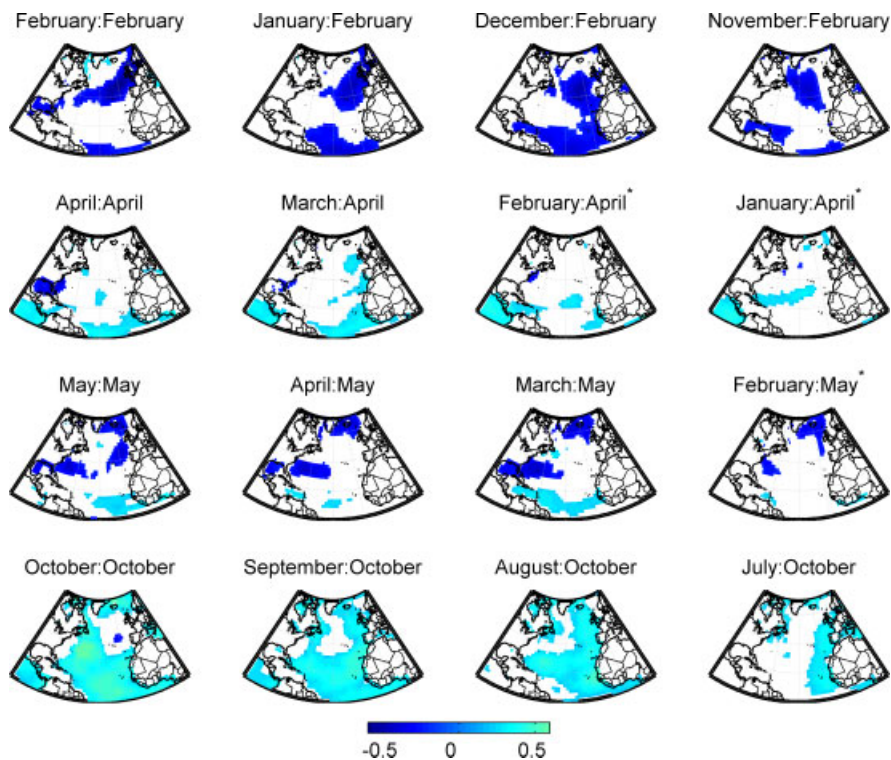


Figure 3. The spatial distribution of significant SSTA: NWIPR (sea surface temperature anomalies: regional index of rainfall) concurrent and lagged correlations. The asterisk corresponds to SSTA: NWIPR correlations that do not satisfy the interdependence criterion. This figure is available in colour online at www.interscience.wiley.com/ijoc

The analysis of lagged SSTA: NWIPR correlation (Figure 3) allows inferring the following results. First, the correlation areas observed for concurrent analysis can still be observed when considering one- and two-monthly lagged NWIPR, although the extent of those areas is slightly reduced. Thus, the bands across the Atlantic observed for concurrent analysis are observed to split into spots. Second, the correlation is observed to decrease and even disappear (the interdependence criterion is not fulfilled) when considering three-monthly lagged NWIPR.

In the following, clusters will be identified using the criterion described in Data and Methods section. Only one- and two-monthly lagged correlations will be considered since the correlation is not amply significant when considering SSTAs three months in advance (Figure 3).

Clusters defined for February are located in the north-east Atlantic area near Ireland and southwest Great Britain, C1, and in the central equatorial Atlantic, C2 (Figure 4). Regression equation containing both clusters and considering one-monthly lagged NWIPR results in a correlation of 0.54. Equations and coefficients are summarised in Table IV. The correlation increases up to 0.58 when considering both clusters and one- and two-monthly lagged NWIPR.

Clusters for April are defined in tropical Atlantic, south of Cape Verde Islands, C2, and in tropical Pacific, south of Mexico, C1 (Figure 4). In this case, correlations have a significant correlation of 0.41 assuming one-monthly lagged NWIPR. This correlation achieves a value of 0.44 considering one- and two-monthly lagged NWIPR.

May clusters are located in front of the eastern coast of the United States, C1, and the area surrounding Iceland, C2 (Figure 4). Correlation values for the regression equations are 0.42 and 0.50 considering one-monthly lagged NWIPR and one- and two-monthly lagged NWIPR, respectively.

Finally, in October, one cluster is located in the area between Canary and Cape Verde Islands, C1, and the other one north of Caribbean Sea, C2 (Figure 4). Correlation values are respectively 0.45 and 0.59 under the conditions described in previous cases.

Figure 5 shows the comparison between real and predicted rainfall anomaly. Predicted values were calculated using equations in Table IV. The best results were obtained in February and October. In general, the variability is lower in the calculated series than in the real one since the appearance of extreme values can also be influenced by nonlinear processes that were not captured by the linear analysis described above. Despite this fact, the obtained results show a significant correlation between SSTA and lagged NWIPR, the correlation is always lower than 0.60, which means that an important part of the variability cannot be explained by a simple linear analysis. Nevertheless, the relationship between both variables can be of some utility to anticipate rainfall anomaly (higher or lower than normal), which can play a key role in different applications such as energy generation or water supply. Thus, a discrete predictand was created assuming only two possible states, namely, rainfall higher or lower than normal. Only values outside the interval $< \text{NWIPR} > \pm 1/2\sigma(\text{NWIPR})$ were considered, since they correspond to those events that can be potentially more harmful, giving rise to floods and droughts. In general, results (Table V) show the accuracy of the method to forecast extreme rainfalls both higher and lower than normal. The worst forecast corresponded to April, where only 76% of the extreme events were properly identified in the contingency table. On the other hand, the best forecast corresponded to February, where 86% of the extreme events were properly identified.

The location and intensity of SSTA spots associated to extreme events can be calculated by means of composite

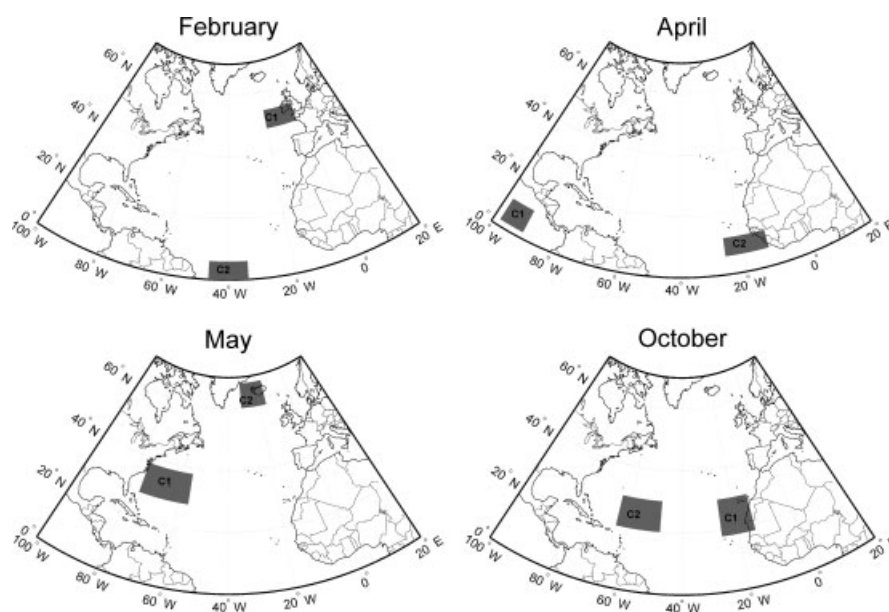


Figure 4. Geographic location of the areas of sea surface temperature that shows higher correlations with the rainfalls of the months of February, April, May and October.

Table IV. Monthly stepwise regression model of rainfall anomaly considering one-monthly lagged NWIPR and considering one- and two-monthly lagged NWIPR.

Month	Lag	Equation	Correlation
February	1 month	NWIPR = $a \times C1(SSTL1) + b \times C2(SSTL1)$ $a = -0.3030, b = -0.3489$	0.5369
	1 and 2 months	NWIPR = $a \times C1(SSTL1) + b \times C2(SSTL1) + c \times C1(SSTL2) + d \times C2(SSTL2)$ $a = -0.3588, b = -0.3389, c = -0.1176, d = 0.2284$	0.5837
April	1 month	NWIPR = $a \times C1(SSTL1) + b \times C2(SSTL1)$ $a = 0.2655, b = 0.1792$	0.4089
	1 and 2 months	NWIPR = $a \times C1(SSTL1) + b \times C2(SSTL1) + c \times C1(SSTL2) + d \times C2(SSTL2)$ $a = -0.0221, b = 0.1475, c = 0.4189, d = -0.0208$	0.4355
May	1 month	NWIPR = $a \times C1(SSTL1) + b \times C2(SSTL1)$ $a = -0.4373, b = 0.0422$	0.4156
	1 and 2 months	NWIPR = $a \times C1(SSTL1) + b \times C2(SSTL1) + c \times C1(SSTL2) + d \times C2(SSTL2)$ $a = 0.0214, b = 0.2428, c = -0.1061, d = -0.0016$	0.5045
October	1 month	Prec = $a \times C1(SSTL1) + b \times C2(SSTL1)$ $a = 0.2102, b = 0.2234$	0.4525
	1 and 2 months	Prec = $a \times C1(SSTL1) + b \times C2(SSTL1) + c \times C1(SSTL2) + d \times C2(SSTL2)$ $a = -0.2310, b = 0.0421, c = 0.4544, d = 0.2823$	0.5862

SSTAs, sea surface temperature anomalies; NWIPR, regional index of rainfall; SST, sea surface temperature; Prec, precipitation.

The input variables were the mean values of SSTA for the two most significant clusters of SSTA: NWIPR correlation fields. C1 and C2 correspond to cluster 1 and cluster 2 obtained for each month. L1 and L2 made reference to 1 month of lag and 2 months of lag, respectively. In this way, in February, C1 (SSTL1) represents the average of the SST of area C1 and C2 (SSTL1) represents the average of the SST of area C2, see Figure 4, with a 1 month of lag and so on.

Table V. Contingency tables using equations in Table IV to forecast extreme rain events.

February	Observed (-)	Observed (+)
Forecasted (-)	10	0
Forecasted (+)	3	8
April	Observed (-)	Observed (+)
Forecasted (-)	8	3
Forecasted (+)	2	8
May	Observed (-)	Observed (+)
Forecasted (-)	10	1
Forecasted (+)	3	7
October	Observed (-)	Observed (+)
Forecasted (-)	9	2
Forecasted (+)	3	9

analysis (Figure 6). SSTA fields corresponding to months under extreme positive (negative) NWIPR events were averaged and then subtracted (positive minus negative events) to obtain composites. The same procedure was followed using lagged SSTA fields, one or two months in advance. Once again, only the months fulfilling the interdependence criterion were considered in this analysis. The obtained composites closely resemble the SSTA

areas strongly correlated with NWIPR (Figure 4) both for concurrent and lagged rainfall. Thus, areas of significant negative (positive) correlation in Figure 4 correspond to negative (positive) values in SSTA composites. Actually, the clusters defined in Figure 5 can be perfectly identified in the composites. The most remarkable difference between SSTA: NWIPR correlation maps and composites appears in February when a positive spot in the lagged composite fields can be observed in the mid-Atlantic at latitudes ranging from 40° to 50°N. This spot had not been previously observed in the correlation field, possibly due to the fact that this region becomes important when considering extreme events, although its importance decreases when considering the entire period as done in correlation analysis.

5. Discussions

In this work, we have investigated the existence of a lagged Pearson's correlation between SSTA in the Atlantic area and a rainfall anomaly index in Galicia (NW Iberian Peninsula). We have applied finiteness and interdependence of the spatial grid criteria to avoid spurious correlations. We found robust and highly significant lagged correlations for February, April, May and October.

The pattern of SSTA in November, December and January related with rainfall in February resembles the well-known tripole pattern, where the lobe located in the east coast of United States is almost negligible. Actually, it

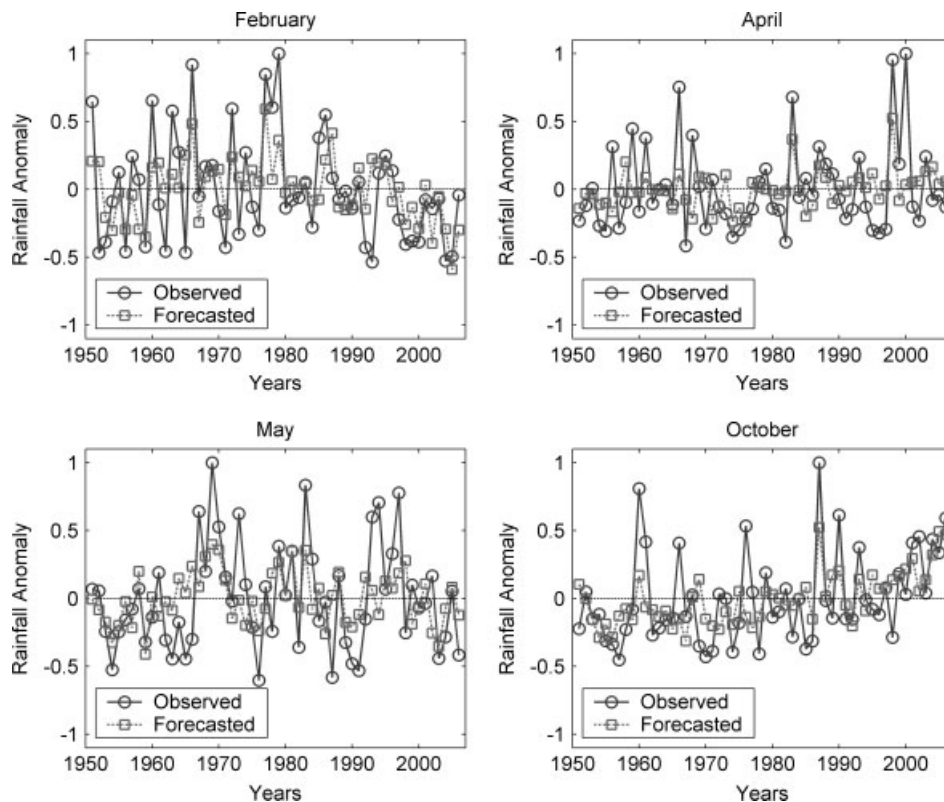


Figure 5. Time series of rainfall anomaly observed (circles) and forecasted (squared) from 1951 to 2006 for the considered months.

can only be observed when significances of 90% are considered. The tripole is the leading pattern of SST variability in the North Atlantic (Czaja and Frankignoul, 1999; Marshall *et al.*, 2001) and has been related with atmospheric circulation, and in particular with North Atlantic Oscillation (NAO) pattern in winter (Czaja and Frankignoul, 2002; Czaja *et al.*, 2003; Cassou *et al.*, 2004b). In particular, the two northern lobes could affect the storm track, while the southern lobe could affect Hadley circulation (Czaja *et al.*, 2003; Losada *et al.*, 2007). Some works have proved the relationship between the southern lobe of this pattern and winter rainfall in the Iberian Peninsula and Northwest Africa (Rodríguez-Fonseca and de Castro, 2002; Rodríguez-Fonseca *et al.*, 2006). This suggests a physical link between February rainfall and SSTA obtained in the precedent months. Negative anomalies in the two lobes contribute to a weakening of semipermanent Azores high and it should thus favour more cold fronts reaching our area. Moreover, location of these anomalies is consistent with the dominance of southwest-erlies and westerlies weather type situations in winter (Lorenzo *et al.*, 2008). The anticorrelation between SSTA in those areas and rainfall in February could be affected by the stability of the air column that is enhanced by cold water, diminishing the activity of cold fronts moving over those areas.

The SSTA pattern in summer (July, August and September) related with rainfall anomalies in October can be related with the horseshoe pattern that appears in this season. Anomalously cold SST southeast of Newfoundland and anomalously warm SST along the eastern

boundary of the Atlantic project a negative phase of NAO some months later (Czaja and Frankignoul, 1999; Drevillon *et al.*, 2001; Cassou *et al.*, 2004a). In our case, the positive correlation with the eastern boundary of the Atlantic suggests that the horseshoe pattern tends to preclude a negative NAO that improve the possibility of rainfall situations in October, when polar jet stream approaches the latitude of Galicia. Moreover, in August and September, the Atlantic warm pool is also positively correlated with rainfall in October. Some works have proven (Wang *et al.*, 2007) that this warm pool tends to reduce the strength of the North Atlantic subtropical high.

The patterns that appear for May and April are not so clear. A plausible explanation is that we are seeing the distortion of the tripole pattern by advection, with no discernible pattern. It is remarkable for April that we have a spot outside the Atlantic, in the Equatorial Pacific area, suggesting a connection between El Niño area and Galicia (NW Spain). This relationship is outside the scope of our work, but will be further studied in following works. It has been suggested that analysis of North Atlantic climate variability must take into account the role of the whole Tropics, including both Pacific and Indian Ocean sectors (Hoerling *et al.*, 2004; Hurrell *et al.*, 2004). On the other hand, the SSTA in March and April that correlates with rainfall in May, suggest a strengthening of the westerlies in response to a strengthening of the meridional SST gradients that has been seen in wintertime (Sutton *et al.*, 2001).

Taking into account the criteria of finiteness and interdependence of the spatial grid, only February, April,

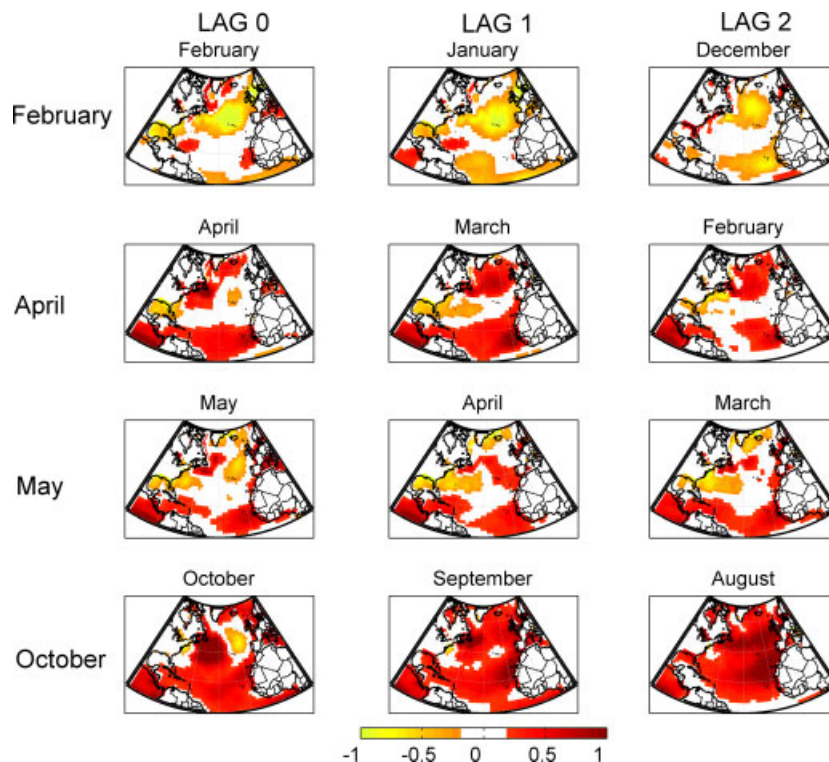


Figure 6. Composite maps. Sea surface temperature anomaly fields corresponding to months under extreme positive (negative) NWIPR (regional index of rainfall) events were averaged and then subtracted (positive minus negative events) to obtain composites. This figure is available in colour online at www.interscience.wiley.com/ijoc

May and October have statistical correlation between SSTA and rainfall. Nevertheless, the reason that this correlation does not appear in other months can be explained when relaxing those criteria. January and February share the same pattern of relationship between SSTA and rainfall. But in the case of January, the pattern is not important enough to surpass the two criteria. The same argument can be used for March. It is a transition month between winter and spring. As explained in the article, correlation of SSTA and rainfall in spring (April and May) is mainly in the tropical Atlantic area, whereas in winter (February), the correlation takes place following the tripole pattern.

The case for summer months (June, July, August and September) is somewhat different. As we can see in Figure 2, rainfall in those months is not very important. Moreover, summer rainfall is not linked with variations at a synoptic scale. Actually, no significant correlation is obtained during these months when correlating annual summer rainfall variability with NAO or other variability modes in the Atlantic area. This means that summer rainfall is mostly provoked by mesoscale phenomena, such as convective cells, and atmospheric and oceanic variability do not have consequences on rainfall in summer. On the other hand, prevalent winds in those months block the possible connection between Atlantic warm pool and the area under study (Wang *et al.*, 2007).

October presents the most outstanding change all over the year. In this month begins the rainiest part of the year. As the heat content of the ocean in the precedent

months is in its higher limit, the influence of the ocean achieves a maximum. In this case, the correlation of SSTA of August and September and rainfall in October takes place over the horseshoe pattern. This influence does not appear in November that plays the same role of January and March, as transitional months among different seasons. The fast changing conditions between different months, characteristic of the area under study, make the election of monthly accumulated rainfall more suitable than seasonal one.

6. Conclusions

This work has investigated links between SST variations in North Atlantic and rainfall in NW Iberian Peninsula. We have taken into account monthly mean correlations between SST and NWIPR from zero to three months of lag. Five months (February, April, May, October and December) were observed to satisfy the finiteness and interdependence criteria for field significance at the 0.1 level for concurrent SSTA: NWIPR although, the interdependence criteria is only satisfied for February, April, May and October for one- and two-monthly lagged analysis. This fact can provide a useful tool to forecast monthly rainfall anomalies in NW Iberian Peninsula. Similar results were obtained by Phillips and McGregor (2002) for southwest England rainfall and Phillips and Thorpe (2006) for Iceland.

The Atlantic areas influencing rainfall in NW Spain were clustered to be used as input variables for rainfall

anomalies forecast. Considering one- or two-monthly lagged regression equations provides correlations up to 0.59 between observed and predicted anomalies. The potential predictability ranges from 76% to 86% when considering extreme episodes of rainfall as a discrete predictand. It should be noticed that NW Spain is a region with important hydroelectric energy productivity and prone to short duration drought. Therefore, it is useful to know the sign of the anomaly 1 month in advance, even if the exact quantity of rain could not be precisely calculated.

Finally, new research should be conducted to study the mechanism involved in the correlations explained in the article, using an atmospheric general circulation model and a regional climate model (RCM). The first one will be used to assess the influence of the SSTA over the circulation affecting the area under study and to provide boundary conditions to the RCM. The RCM itself will provide the physical link between SSTA and rainfall, because general circulation models have difficulties with the distribution of precipitation and a dynamical downscaling will be needed. Moreover, dynamical links should also be explored to explain the relationship between SST and rainfall that persist more than three months, such as the so-called re-emergence mechanism (Cassou *et al.*, 2007).

Acknowledgements

This work is supported by 'Xunta de Galicia' underproject PGIDIT06PXIB383288PR. J. J. Taboada acknowledges the financial support from the Department of Environment of the Galician Government (Xunta de Galicia). M. N. Lorenzo acknowledges the support by the Ramón y Cajal program.

References

- Alvarez I, deCastro M, Gómez-Gesteira M, Prego R. 2005. Inter- and intra-annual analysis of the salinity and temperature evolution in the Galician Rias Baixas-ocean boundary (northwest Spain). *Journal of Geophysical Research* **110**: 1–14. C04008. DOI:10.1029/2004JC002504.
- Alvarez I, Gomez-Gesteira M, deCastro M, Novoa EM. 2008. Ekman transport along the Galician Coast (NW, Spain) calculated from QuikSCAT winds. *Journal of Marine Systems* **72**(1–4): 101–115.
- Barnston AG. 1994. Linear statistical short-term climate predictive skill in the Northern Hemisphere. *Journal of Climate* **7**: 1513–1564.
- Barnston AG, Smith TM. 1996. Specification and prediction of global surface temperature and precipitation from global SST using CCA. *Journal of Climate* **9**: 2660–2697.
- Cabanas JM, Alvarez I. 2005. Ekman transport patterns in the area close to the Galician coast (NW, Spain). *Journal of Atmospheric and Ocean Science* **10**(4): 325–341.
- Cassou C, Deser C, Alexander MA. 2007. Investigating the impact of reemerging sea surface temperature anomalies on the winter atmospheric circulation over the North Atlantic. *Journal of Climate* **20**: 3510–3526.
- Cassou C, Deser C, Terray L, Hurrell JW, Drévilion M. 2004a. Sea surface temperature conditions in the North Atlantic and their impact upon the atmospheric circulation in early winter. *Journal of Climate* **17**: 3349–3363.
- Cassou C, Terray L, Hurrell JW, Deser C. 2004b. North Atlantic winter climate regimes: spatial asymmetry, stationarity with time, and oceanic forcing. *Journal of Climate* **17**: 1055–1068.
- Czaja A, Frankignoul C. 1999. Influence of the North Atlantic SST on the atmospheric circulation. *Geophysical Research Letters* **26**(19): 2969–2972.
- Czaja A, Frankignoul C. 2002. Observed impact of Atlantic SST anomalies on the North Atlantic Oscillation. *Journal of Climate* **15**: 606–623.
- Czaja A, Robertson W, Huck T. 2003. The role of Atlantic Ocean-atmosphere coupling in affecting North Atlantic oscillation variability. *The North Atlantic Oscillation: Climate Significance and Environmental Impact, Geophysical Monograph Series, 134*, Hurrell JW, Kushnir Y, Ottersen G, Visbeck M (eds) American Geophysical Union: Washington, DC; 147–172.
- deCastro M, Gómez-Gesteira M, Álvarez I, Lorenzo MN, Cabanas JM, Prego R, Crespo AJC. 2008a. Characterization of fall–winter upwelling recurrence along the Galician western coast (NW Spain) from 2000 to 2005: dependence on atmospheric forcing. *Journal of Marine Systems* **72**(1–4): 145–158.
- deCastro M, Gómez-Gesteira M, Lorenzo MN, Álvarez I, Crespo AJC. 2008b. Influence of atmospheric modes on coastal upwelling along the western coast of the Iberian Peninsula, 1985 to 2005. *Climate Research* **36**: 169–179.
- deCastro M., Lorenzo MN, Taboada JJ, Sarmiento M, Álvarez I, Gómez-Gesteira M. 2006. Influence of teleconnection patterns on precipitation variability and on river flow regimes in the Miño River basin (NW Iberian Peninsula). *Climate Research* **32**: 63–73.
- Delitala AMS, Cesari D, Chessa PA, Ward MN. 2000. Precipitation over Sardinia (Italy) during the 1946–1993 rainy seasons and associated large scale climate variations. *International Journal of Climatology* **20**: 519–541.
- Drévilion M, Terray L, Rogel P, Cassou C. 2001. Midlatitude Atlantic SST influence on European winter climate variability in the NCEP reanalysis. *Climate Dynamics* **18**: 331–344.
- Frankignoul C, Czaja A, L'Heveder B. 1998. Air–sea feedback in the North Atlantic and surface boundary conditions for ocean models. *Journal of Climate* **11**: 2310–2324.
- Gomez-Gesteira M, Moreira C, Álvarez I, deCastro M. 2006. Ekman transport along the Galician coast (northwest Spain) calculated from forecasted winds. *Journal of Geophysical Research* **111**: C10005. DOI:10.1029/2005JC003331.
- Hoerling MP, Hurrell JW, Xu T, Bates GT, Phillips AS. 2004. Twentieth century North Atlantic climate change. Part II: understanding the effect of Indian Ocean warming. *Climate Dynamics* **23**: 391–405.
- Hurrell JW, Hoerling MP, Phillips AS, Xu T. 2004. Twentieth century North Atlantic climate change. Part I: assessing determinism. *Climate Dynamics* **23**: 371–389.
- Livezey RE, Chen WY. 1983. Statistical field significance and its determination by Monte Carlo techniques. *Monthly Weather Review* **111**: 46–59.
- Lorenzo MN, Taboada JJ. 2005. Influences of atmospheric variability on freshwater input in Galician Rías in winter. *Journal of Atmospheric and Ocean Science* **10**(4): 377–387.
- Lorenzo MN, Taboada JJ, Gimeno L. 2008. Links between circulation weather types and teleconnection patterns and their influence on precipitation patterns in Galicia (NW Spain). *International Journal of Climatology* **28**: 1493–1505.
- Losada T, Rodríguez-Fonseca B, Mechoso CR, Ma HY. 2007. Impacts of SST anomalies on the North Atlantic atmospheric circulation: a case study for the northern winter 1995/1996. *Climate Dynamics* **29**: 807–819, DOI: 10.1007/s00382-007-0261-x.
- Marshall J, Kushnir Y, Battisti D, Chang P, Czaja A, Dickson R, McCartney M, Saravanan R, Visbeck M. 2001. North Atlantic climate variability: phenomena, impacts and mechanisms. *International Journal of Climatology* **21**: 1863–1898.
- Martínez Cortizas A, Pérez Alberti A. 2000. Atlas climático de Galicia. Centro de información e tecnoloxía ambiental. Desenvolvemento sostible. Xunta de Galicia. <http://biblioteca.climantica.org/resources/210/atlas.pdf>.
- Peterson ThC, Vose R, Schmoyer R, Razuvaev V. 1998. Global historical climatology network (GHCN) quality control of monthly temperature data. *International Journal of Climatology* **18**: 1169–1179.
- Phillips ID, McGregor GR. 2001. Western European water vapor flux–Southwest England rainfall associations. *Journal of Hydrometeorology* **5**: 505–523.
- Phillips ID, McGregor GR. 2002. The relationship between monthly and seasonal south-west England rainfall anomalies and concurrent North Atlantic sea surface temperatures. *International Journal of Climatology* **22**: 197–217.

- Phillips ID, Thorpe J. 2006. Icelandic precipitation-North Atlantic sea-surface temperature associations. *International Journal of Climatology* **26**: 1201–1221.
- Rodriguez-Fonseca B, de Castro M. 2002. On the connection between winter anomalous precipitation in the Iberian Peninsula and Morocco and the summer subtropical Atlantic SST. *Geophysical Research Letters* **29**(18): 1863. DOI:10.1029/2001GL014421.
- Rodriguez-Fonseca B, Polo I, Serrano E, Castro M. 2006. Evaluation of the North Atlantic SST forcing on the European and Northern African winter climate. *International Journal of Climatology* **26**: 179–191.
- Rodwell MJ, Folland CK. 2002. Atlantic air–sea interaction and seasonal predictability. *Quarterly Journal of the Royal Meteorological Society* **128**: 1413–1443.
- Rodwell MJ, Rowell DP, Folland CK. 1999. Oceanic forcing of the wintertime North Atlantic Oscillation and European climate. *Nature* **398**: 320–323.
- Rowell DP. 1998. Assessing potential seasonal predictability with an ensemble of multidecadal GCM simulations. *Journal of Climate* **11**: 109–120.
- Sutton R, Norton W, Jewson S. 2001. The North Atlantic Oscillation – what role for the ocean? *Atmospheric Science Letters* **1**: 89–100.
- Wang C, Lee S-K, Enfield DB. 2007. Impact of the Atlantic warm pool on the summer climate of the western hemisphere. *Journal of Climate* **20**(20): 5021–5040.
- Wilks DS. 1995. *Statistical Methods in the Atmospheric Sciences: An Introduction, International Geophysics Series, 59*. Academic Press: San Diego, CA; 464.